Available online at www.sciencedirect.com
ScienceDirect
International Journal of Heat and Mass Transfer 51 (2008) 1332–1341
International Journal of HEAT and MASS TRANSFER
www.elsevier.com/locate/ijhmt

Natural convection of microparticle suspensions in thin enclosures

B.H. Chang [1], A.F. Mills *, E. Hernandez

Mechanical and Aerospace Engineering Department, University of California, Los Angeles, CA 90095, United States

Received 14 March 2007; received in revised form 18 August 2007
Available online 25 January 2008

Abstract

Natural convection experiments were performed with aluminum oxide microparticle aqueous suspensions in thin enclosures of circular planform at angles of inclination to the horizontal of 90°, 30° and 0°. The average size of the aluminum oxide particles was about 250 nm, and volume fractions of 1.31% and 2.72% were used. The aspect ratio varied from 50.7 to 10.9, and the maximum Raleigh number was 3×10^5. No effect of particles on the Nusselt number–Rayleigh number relation was found for the vertical enclosure at 90°. However at 30° and 0° (horizontal) there was a decrease in Nusselt number compared to pure water, which was pronounced at lower Rayleigh number and higher particle concentrations. This anomalous behavior is attributed to sedimentation.
© 2007 Elsevier Ltd. All rights reserved.

Keywords: Natural convection; Microparticle; Sedimentation; Thermophoresis

1. Introduction

Convective heat transfer in nanofluids has received much attention in recent years. Stable suspensions of nanosize particles have been developed, and these nanofluids have been found to often have anomalously high thermal conductivities. There have been numerous experimental studies to determine convective heat transfer coefficients, in the hope that use of nanofluids will prove to be a viable way to increase convective heat transfer. Unfortunately, the current literature is characterized by contradictory experimental data, and much controversy as to the physical mechanisms of heat transfer enhancement. Also, seldom put in the proper context is the fact that the increased viscosity of the nanofluid can negate gains due to increased thermal conductivity when a proper thermal-hydraulic design is executed.

Most experimental results for convective heat transfer in nanofluids have been obtained for forced convection, usually inside tubes. Few experimental studies of natural convection have been reported [1–3]. Although the titles of the papers refer to "nanofluids" the average particle sizes were in the range 80–170 nm and are more correctly described as microparticle suspensions. We report an experimental study of natural convection in a thin enclosure of circular planform at various inclinations to the horizontal. The nanofluids used were aluminum oxide particles in water at 5% and 10% by weight (volume fractions of 1.31% and 2.72%). The primary particle size was less than 20 nm as specified by the manufacturer, but due to agglomeration the effective particle size was about 250 nm.

2. Previous work

The most significant studies of natural convection in a thin enclosure are those of Wen and Ding [1,2], who used a horizontal enclosure 10 mm high and 24 cm in diameter. The test fluids were suspensions of titanium dioxide particles in water with an average agglomerate size of 170 nm. In their later study, the concentrations were 0.8%, 1.5% and 2.5% by volume. They found decreasing heat transfer coefficients with increasing particle concentrations. Care must be taken in examining their results. In Ref. [1] they

* Corresponding author. Tel.: +1 310 825 3583; fax: +1 310 206 4830.
E-mail address: amills@seas.ucla.edu (A.F. Mills).
[1] On Leave from Department of Computer Aided Mechanical Design, Incheon City College, Incheon 402-750, South Korea.

0017-9310/$ - see front matter © 2007 Elsevier Ltd. All rights reserved.
doi:10.1016/j.ijheatmasstransfer.2007.11.030

Nomenclature

AR	aspect ratio
c_P	specific heat at constant pressure, J/kg K
d_P	particle diameter
D	Brownian diffusion coefficient
D_T	thermal diffusion coefficient
g	gravitational acceleration
h	heat transfer coefficient, W/m^2 K
H	channel height, m
k	thermal conductivity, W/m K
n	particle number density
Nu	Nusselt number
q	heat flux, W/m^2
Ra	Raleigh number, $\rho\beta\Delta TH^3/\mu\alpha$
T	temperature, K
t	time
V_P	particle volume
v_S	sedimentation velocity, m/s
v_T	thermophoretic velocity, m/s
z	vertical coordinate

Greek symbols

α	thermal diffusivity, m^2/s
β	$(v_S + v_T)H/D$ or thermal expansion coefficient, 1/K
μ	dynamic viscosity, Pa s
ν	kinematic viscosity, m^2/s
ρ	density, kg/m^3
η	z/H
ϕ	volume concentration
θ	inclination angle

Subscripts

C	cold side
H	hot side
l	liquid
p	particle
s	sedimentation
T	thermophoresis
–	average value

did not measure the thermal conductivity and viscosity of their suspensions, and when calculating Nusselt and Rayleigh numbers used pure water properties. In Ref. [2] they did report measurements of conductivity and viscosity, but did not use these data when calculating Nusselt and Rayleigh numbers. Thus their key figures of Nusselt number versus Rayleigh number are, in effect, plots of heat transfer coefficient versus temperature difference, and indeed show decreased heat transfer coefficients with increasing particle concentrations. In their discussion they claim that the decrease could not be attributed to changes in transport properties.

Putra et al. [3] investigated natural convection in a cylindrical cavity with its axis horizontal and heated on one end, cooled at the other end. Aspect ratios of 0.5, 1.0 and 1.5 were used. The test fluids were aqueous suspensions of Al_2O_3 and CuO particles at 1% and 4% concentration by volume. The volume weighted average values of particle diameter were 131.2 and 87.3 nm for Al_2O_3 and CuO, respectively. They measured the viscosities and thermal conductivities of the test suspensions, and used these properties to calculate the Nusselt and Rayleigh numbers. An unexpected decrease in Nusselt numbers at fixed Rayleigh numbers with increasing particle concentration was found. Since the measured properties were used in the dimensionless groups, the conclusion is that there were phenomena associated with the particles that are not accounted for in the measured transport properties. Furthermore, the corresponding decrease in heat transfer coefficients at fixed temperature difference were even larger.

A numerical study of natural convection in a two-dimensional enclosure containing a nanofluid has been reported by Khanafer et al. [4], and these authors obtain increased heat transfer coefficients with increasing particle concentrations. However this feature results from including a thermal dispersion term to augment heat conduction. The thermal dispersion term is of a form derived for convection in porous solids and contains an unspecified multiplying constant. Since the particles move with the fluid in the numerical model, it is difficult to accept that the thermal dispersion term is meaningful: the increased heat transfer rates claimed are simply the result of using an increased thermal conductivity (over and above the value for a stagnant nanofluid).

In summary, the previous experimental works show an unexpected and unexplained decrease in natural convection heat transfer coefficients with increasing particle concentrations for microparticle suspensions. We will report comprehensive data that will show no effect of microparticles on natural convection Nusselt versus Rayleigh number relations in thin enclosure oriented at 90° to the horizontal. We will also present data showing decreased Nusselt numbers at horizontal and 30° inclinations, particularly at lower Rayleigh numbers, which will be attributed to sedimentation. An analysis will be presented that explains the effect of sedimentation and thermophoresis on the possible stability of a horizontal fluid layers.

3. Test fluids

The Al_2O_3 nanofluids used in the present study were 5 wt% and 10 wt% dispersion in water and were supplied by the Sigma–Aldrich Co. The corresponding particle volume fractions were 1.31% and 2.72%. The manufacturer claimed an average size of the nanoparticles of 20 nm, but measurements with the Brookhaven Instruments

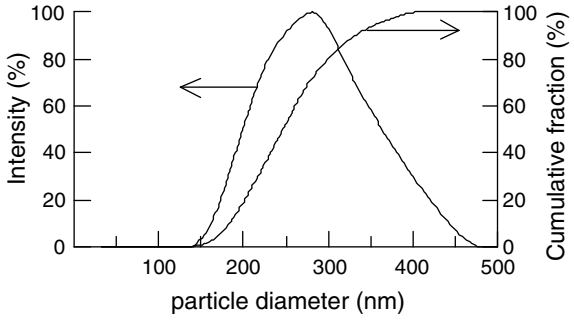

Fig. 1. Typical size distribution of particles.

Corporation 90Plus/BI_MAS Option particle sizer that uses a laser light intensity scattering technique showed an effective diameter of about 250 nm. The effective diameter was unaffected by sonication. The difference in the particle size between the manufacturer's claim and our measurements is attributed to agglomeration of the nanoparticles. The Brookhaven instrument used in this study is capable of measuring sizes from 2 nm to 3 μm. Fig. 1 shows a typical particle distribution obtained with the instrument. A similar discrepancy can be seen in the work of Wen and Ding [1] who showed that the average particle size of the titanium dioxide particles was 170 nm, even though the nominal size from the manufacturer was 34 nm. Wen and Ding [1] used a scanning electron microscope, which requires evaporation of the fluid specimen to obtain dried particles for measurements. Thus the actual size of dispersed particles in solution was not measured.

The thermal conductivities of the test fluids were measured in two ways. One method was from a pure conduction experiment with the fluid, in which the top plate of the test cell was heated and the bottom cooled. Knowing the heat flux through the fluid, the effective thermal conductivity of the fluid can be calculated. The second method was the transient hot-wire technique: the difference in thermal conductivity by the two methods was less than 0.3%. The measured effective thermal conductivities were 0.614 and 0.629 W/m K for 5 wt% and 10 wt% at 21.5 °C. The thermal conductivity of the fluid sample was measured 2 months after a set of experiments was completed, and the change was about 0.6%. The thermal conductivity measured by Zhang et al. [5] for 10 wt.% Al_2O_3 from Sigma–Aldrich Co. was about 0.64 W/m K. This is about 1.7% higher than the measured value in this study.

The density of the suspension was evaluated by using the following relation:

$$\rho = (1-\phi)\rho_{\mathrm{l}} + \phi\rho_{\mathrm{P}} \tag{1}$$

The density and specific heat product was determined from

$$\rho c_P = (1-\phi)(\rho c_P)_{\mathrm{l}} + \phi(\rho c_P)_{\mathrm{P}} \tag{2}$$

With Eq. (2), the expression for the effective thermal diffusivity becomes

$$\alpha = \frac{k}{(1-\phi)(\rho c_P)_{\mathrm{l}} + \phi(\rho c_P)_{\mathrm{P}}} \tag{3}$$

Viscosity data for nanofluids are sparse. Putra et al. [3] reports $\mu \approx 1.16 \times 10^{-3}$ Pa s for 131.2 nm Al_2O_3 particles at $\phi = 1\%$. A much larger viscosity was measured by Pak and Cho [6] for 13 nm Al_2O_3 particles at $\phi = 1.34\%$, of 1.65×10^{-3} Pa s at a shear rate of 395 s^{-1}. In this study, the viscosity was measured by a capillary tube viscometer, and the values obtained were 1.29×10^{-3} and 1.88×10^{-3} Pa s for 1.31% and 2.72%, respectively. The viscometer was first checked by measuring the viscosity of pure water.

4. Experimental apparatus and procedure

The cylindrical experimental apparatus of the present study is schematically shown in Fig. 2. The test fluid is contained between two 15.2 cm diameter copper plates, each 1.58 mm thick. Behind each copper plate is a layer of RTV 630 to serve as a heat flux meter, with copper blocks located behind each heat flux meter. The copper plates and the heat flux meters are contained inside a 9.5 mm thick plexiglass cylinder. Heated water is circulated inside the hot side copper block, and its temperature is controlled by an electric heater. The cold copper block is cooled by a glycol coolant that is circulated through a heat exchanger to reject heat to a refrigerator. A total of 20 thermocouples are located in shallow grooves in the copper plates on either side of the heat flux meters, and they are connected to a data acquisition system which samples the emf signals at 10 Hz frequency. The output is transmitted to a computer for averaging, differencing, and display. The cold plate assembly can be moved to change the fluid layer thickness, which is measured using a dial gage. The entire test section is mounted on steel shafts and can be rotated from 0°(heated from below) to 180°(heated from above). The test fluid layer is maintained at an average temperature equal to the ambient temperature. Steady state was attained about 3 h after the entire apparatus was switched on.

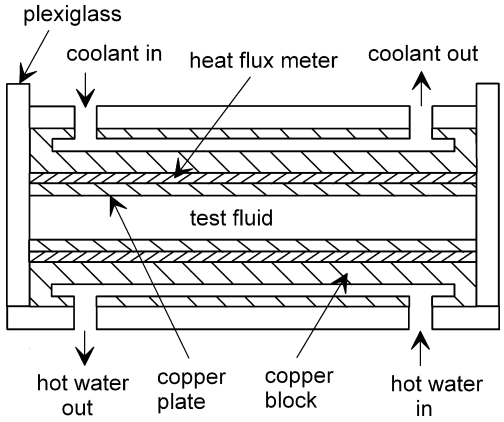

Fig. 2. Schematic diagram of the experimental apparatus.

The experimental rig (test cell, cooling and heating fluid loops) was allowed to come to an initial steady state. Then the test fluid was mixed thoroughly by filling and emptying the test section repeatedly (the cold plate assembly is mounted on a screw thread drive that allows the gap to be opened and closed rapidly). After 10 min, temperatures were recorded at fixed time intervals. The data were recorded up to 10 h when fluctuations in heat transfer were observed or suspected. Sedimentation was not observed during the experiments, but the suspension was mixed again thoroughly before taking new measurements.

In order to calibrate the heat flux meters a model was used in which the total heat transfer through the heat flux meter was assumed equal to the sum of heat transfer in the fluid, heat conduction in the plexiglass wall, and heat exchange with the environment. The resulting formulas are given in [7], where it was noted that the calculated experimental Nusselt numbers for a horizontal layer of water agreed well with the benchmark data of Rossby [8] and Hollands et al. [9] (typically within 5%, at worst a 9.8% discrepancy with Rossby [8] at very low Rayleigh numbers (4000–7000)). The random error analysis discussed in [7] showed errors in Nusselt number of 12.9% at $H = 2$ mm and 5.7% at $H = 20$ mm which are in line with the observed scatters in the graphed results. It must be emphasized that all the observations and conclusions reached in the current study are based on comparisons with pure water results at equivalent parameter values. Thus any bias errors due to the experimental system are not an issue. Similarly, our methods for measuring the test fluid thermal conductivity and viscosity were benchmarked by measuring values for pure water. The Nusselt number is determined from

$$Nu = \frac{qH}{k\Delta T} \tag{4}$$

where ΔT is the temperature difference across the fluid layer of thickness H.

5. Results and discussion

The major results of this experimental study are given in the form of graphs of Nusselt number versus Rayleigh number. The variation in Rayleigh number was essentially obtained by varying the plate spacing in the range 3–14 mm (aspect ratio 50.7–10.9). The results for angles of inclination equal to 90°, 30° and 0° are shown as Figs. 3–5, respectively, together with results obtained for pure water in a previous study [7]. The Nusselt numbers are steady state asymptotes. At 90° steady values were obtained in relatively short times, of the order of 20 min, but at $\theta = 0°$, times as long as 200 min. were required to obtain the steady values shown. The initial transient behavior of the Nusselt number will be discussed later. Also, for some parameter values, the Nusselt number oscillated around a steady mean value asymptote: this behavior will also be discussed later.

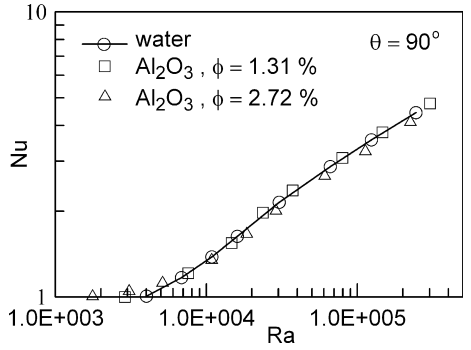

Fig. 3. Nusselt number results for vertical fluid layer.

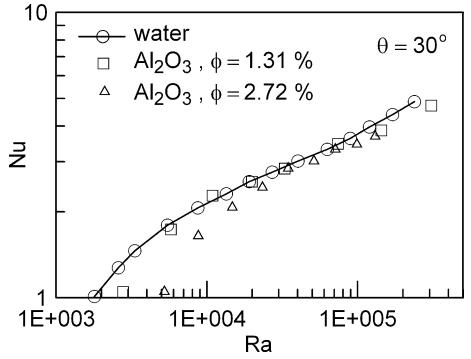

Fig. 4. Nusselt number results for fluid layer at inclination of 30°.

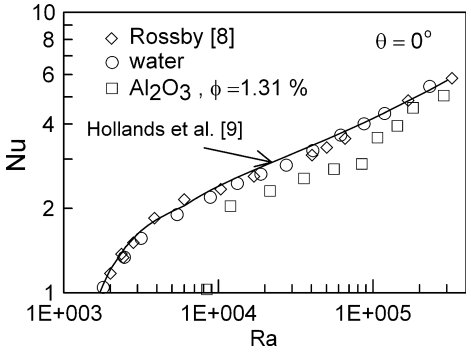

Fig. 5. Nusselt number results for horizontal fluid layer.

It is convenient to first discuss Fig. 3 for $\theta = 90°$ where the gravity vector is perpendicular to the imposed temperature gradient. It appears that there is no significant effect of the particles on the Nusselt–Rayleigh relation. These dimensionless numbers were calculated using thermodynamic and transport properties of the suspensions: thus there is no anomalous heat transfer behavior that can be attributed to the particles. In contrast, Fig. 4 for $\theta = 30°$ shows that the critical Rayleigh numbers are higher than those for water, and the Nusselt numbers are lower, particularly at lower Rayleigh numbers. Fig. 5 for $\theta = 0°$ shows data only for the 1.31% suspension, and the features seen at $\theta = 30°$ are seen to be more marked, that is, a higher critical Rayleigh number, and lower Nusselt numbers over the

whole Rayleigh number range (compared to water). Fig. 5 also shows experimental data for water obtained by Rossby [8], and the correlation of Hollands et al. [9]. The good agreement of our water data with these workers give credibility to our results.

We attribute the anomalous results at $\theta = 30°$ and $\theta = 0°$ to the effects of particle sedimentation. Useful insight was obtained by analyzing the effect of sedimentation on stabilization of the fluid layer. Appendix A presents an analysis of the steady state of a stationary suspension at $\theta = 0°$, and considers particle transport by sedimentation, thermophoresis and Brownian diffusion. For conditions pertinent to our experiments the density gradient is positive at all heights for particle sizes less than ~110 nm, due to the dominant effect of thermophoresis towards the cold plate. Thus particle transport is destabilizing for nanoparticles. For somewhat larger particles sedimentation dominates and the density gradient is negative at all heights giving a stable layer. For microparticles larger than ~120 nm the density gradient is negative at lower elevations but becomes positive at higher elevation. This is the case for our ~250 nm microparticles: indeed sedimentation drives the particles very close to the hot plate, and the layer is essentially pure water with a positive density gradient due to thermal contraction. The layer is unstable with a critical Rayleigh number based on water properties not too different to 1708.

The idea that sedimentation of microparticles can have a stabilizing effect on natural convection in a horizontal enclosure is easily understood. However, in actual experiments, the situation is much more complicated owing to the effect of initial conditions, the wide range of time scales characterizing the various transport phenomena, and the thermal response of the experimental system. The time scales of the transport phenomena are given in Table A.2. For microparticles in our size range the time scale for sedimentation is ~20 h. If the layer is allowed to stand isothermal for times of this order before the plate temperatures are changed, the layer will be unstable with a critical Rayleigh number based on water properties of about 1700, as explained above. However, in our "base" set of tests at $\theta = 0°$ and a particle volume fraction of $\phi = 1.31\%$, an attempt was made to have a near uniform initial concentration of particles throughout the layer by expelling and injecting the test fluid into the cell about 10 times while the plates were heated and cooled as if running a test. Data acquisition commenced about 10 min later. Since Table A.2 shows a time scale for vorticity diffusion of about 0.5 min, initial bulk motion due to the injection of fluid will have damped out after a few minutes. Table A.2 shows a time scale of about 5 min. for thermal diffusion, which characterizes the establishment of a linear temperature profile if the layer remains stable. However the experimental system has a thermal response time scale that can be somewhat longer than 5 min, which can also affect the initial transient behavior of the layer. If the layer remains stable, sedimentation will commence to drive particles towards the bottom of the test cell. Although the time scale for sedimentation is long at ~10 h, an initially uniform particle concentration can decay sufficiently to reverse the density gradient in a much shorter time. Eq. (1) for the suspension density can be differentiated to obtain

$$\frac{d\rho}{dz} = (\rho_P - \rho_l)\frac{d\phi}{dz} + (1-\phi)\rho_l\beta\frac{dT}{dz} \tag{5}$$

Taking $\bar{\phi} = 1.31\%$, $\overline{T} = 293$ K, $\rho_P = 3970$ kg/m^3 gives

$$\frac{d\rho}{dz} \approx 3000 \times \frac{d\phi}{dz} + 0.2 \times \frac{dT}{dz} \tag{6}$$

For $d\rho/dz = 0$ at $\Delta T = 10$ K, $\Delta\phi = 6.7 \times 10^{-4}$, $\Delta\phi/\phi = 0.05$. That is 5% change in ϕ is sufficient to reverse the density gradient (for $\bar{\phi} = 2.72\%$, a 2.5% change is sufficient). Based on a linear response for a small change in ϕ, an order of magnitude estimate of the time required is $(0.05)(10) = 30$ min.

Fig. 6 shows the approach of Nusselt numbers to unity for selected tests at small plate spacing and 0°. The times required are between 30 and 200 min, in line with the value of 30 min deduced from Eq. (6). This agreement suggests that the approach to stability is indeed determined by sedimentation. Also, the approach to stability for the higher $\bar{\phi} = 2.72\%$ is more rapid, also in line with Eq. (6). However the approach behavior appears to be sensitive to the initial conditions, and these need care to control precisely. The test results in Fig. 6 were chosen to illustrate the possible effects of initial conditions on the approach of Nusselt number to unity. We did not observe particle deposition in the time scale of our experiments. The fact that Nusselt numbers did not fall below unity at low Rayleigh numbers confirms an absence of deposition: with significant deposition the fluid conductivity would decrease and yield an apparent Nusselt number less than unity. The Nusselt number is always substantially greater than unity at shorter times. For times larger than the thermal time scales of order 10 min, this behavior is attributed to natural convection mixing damped out by sedimentation: however, flow visualization studies may be necessary to confirm this hypothesis.

Fig. 7 shows the initial transients for $\bar{\phi} = 1.31\%$ and $\theta = 0°$ at larger plate spacings. The duration of the initial

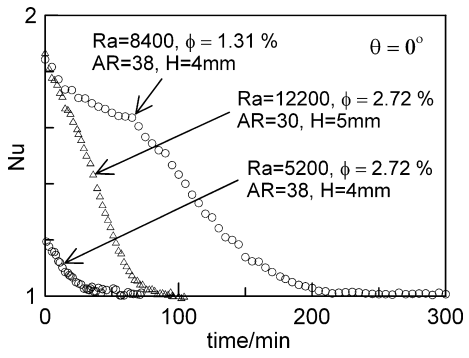

Fig. 6. Nusselt number results at narrow spacings.

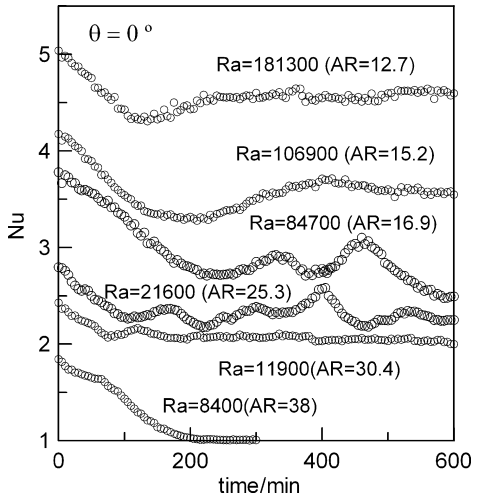

Fig. 7. Nusselt number results for $\phi = 1.31\%$ at various aspect ratio.

transient remains at about 200 min, but now the Nusselt number behavior is more complicated. For plate spacings of 6–9 mm ($Ra = 21{,}600$–$84{,}700$, AR = 25.3–16.9) marked oscillations are in evidence, and a steady asymptote is not attained even after 10 h. For plate spacings of 10–12 mm ($Ra = 106{,}900$–$181{,}300$, AR = 15.2–12.7) there are undershoots in Nusselt number between 100 and 200 min, but then a steady Nusselt number is attained. Since pure water tests show no such oscillations we conclude that the oscillations result from sedimentation alternately stabilizing and destabilizing the thermal boundary layer. Similar oscillations were observed at some plate spacings for the enclosure inclined at 60°. Okada and Suzuki [10] also found Nusselt number oscillations when using much larger particles (4.75 and 6.51 μm average sizes), which appeared to damp out at longer times.

Based on the foregoing discussion of the role played by sedimentation in increasing critical Rayleigh numbers and causing Nusselt number oscillation, we also believe that the anomalously low Nusselt numbers (compared to water) seen in Figs. 4 and 5 result from sedimentation stabilizing the thermal boundary layer at the heated plate. Note that at $\theta = 30°$ in Fig. 4, the reductions are much greater for $\bar{\phi} = 2.72\%$ versus $\bar{\phi} = 1.31\%$. However, without flow visualization or numerical studies, we are unable to give more insight into the pertinent fluid mechanics.

The experiments of Putra et al. [3] with average particle sizes of 87.3 and 131.2 nm were reviewed in the Introduction. Aspect ratios were 0.5–1.5, much smaller than in our experiments (11–38), which gave Rayleigh numbers of 10^6–10^9, which are much larger than in our experiments ($<3 \times 10^5$). Contrary to our results for a narrow enclosure versus a wide enclosure, the Nusselt numbers were lower than those for water. The authors suggest that the cause could be particle-fluid slip and sedimentation. Our results were for much lower Rayleigh numbers which might be pertinent, however, their discrepancy was higher at lower Rayleigh numbers. Experiments with appropriate ranges of aspect ratio, particle size and Rayleigh number are required in order to make further progress.

The experiments of Wen and Ding [1,2] at $\theta = 0°$ with TiO_2 particles at average size 170 nm were also reviewed in the Introduction. Their Nusselt numbers were calculated using pure water properties, and thus should be viewed as heat transfer coefficients versus essentially ΔTH^3. They found decreasing heat transfer coefficients with increasing particle concentrations. In Reference [2] they did report measurements of conductivity and viscosity of the suspensions, and state that the difference in properties was not sufficient to explain the lower heat transfer coefficients. However, it would not be worthwhile to try to improve their data processing for another reason: their steady heat transfer results were generally taken to be values at ~40 min. Examination of Fig. 7 shows that it is unlikely that a true steady state was obtained. Fig. 8 shows the same plots of AR = 25.3 and 16.9 in Fig. 7 for up to 45 min only. Clearly, one could incorrectly assume that the Nusselt numbers have reached a steady value.

Our final comments concern the engineering relevance of the available data for heat transfer by natural convection in enclosure of microparticle suspensions. In all the reported tests, the heat transfer coefficients are lower than those for water at the same parameter values. At best, when the Nusselt number versus Rayleigh number relation is the same as that for water, the heat transfer coefficients are lower due to the greatly increased viscosity of the microparticle suspensions. Fig. 9 shows heat transfer coefficient versus ΔTH^3 for our results at $\theta = 90°$ to illustrate this point. For nanoparticles of size ~10 nm, there may

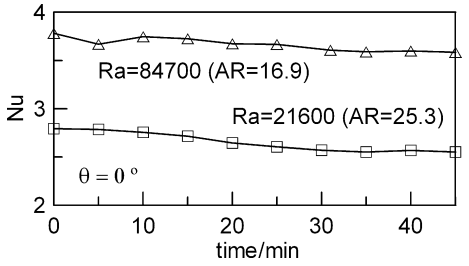

Fig. 8. Nusselt number results at various aspect ratio up to 45 min.

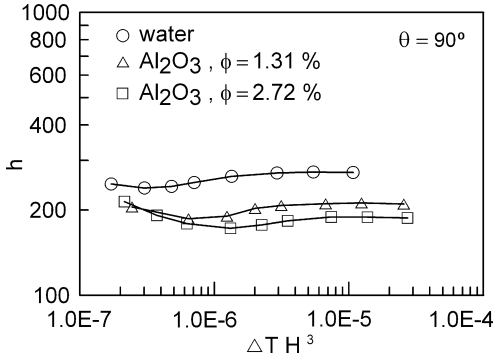

Fig. 9. Heat transfer coefficients vs. ΔTH^3 for vertical fluid layer.

be physical phenomena that increase the effective thermal conductivity dramatically to give improved heat transfer, but no such data appear to exist for natural convection.

6. Conclusions

1. For narrow vertical enclosures there was no effect of microparticles on the Nusselt number–Rayleigh number relation.
2. For narrow enclosures at 0° (horizontal) and 30°, there was a decrease in Nusselt numbers compared to pure water, which was more pronounced at lower Rayleigh numbers and higher particle concentrations.
3. The anomalous heat transfer behavior observed is attributed to sedimentation, which plays an important role for particle sizes greater than ~110 nm at our test conditions.
4. For particle sizes less than ~100 nm, thermophoresis can be expected to play a more important role than sedimentation, and similar anomalies are not expected.

Acknowledgements

Professor E.M.V.Hoek and Anna Jawor facilitated the use of the Brookhaven BI_MAS Option to measure particle size distributions. Professor Y.S. Ju and Ming-Tsung Hung facilitated the use of the transient hot-wire apparatus to measure thermal conductivity. Development Engineer Dale Cooper maintained the data acquisition system. Everardo Hernandez was supported by the UCLA Center for Excellence and Diversity (CEED) under the RISE-UP program. This assistance is gratefully acknowledged.

Appendix. Stability of a horizontal colloidal suspension

Previous work on natural convection of nanofluids has explicitly or implicitly assumed a uniform particle concentration in the fluid, although the possibility of particle sedimentation has been mentioned. The increase in critical Rayleigh number for onset of convection in a horizontal layer shown in Fig. 5 suggests the possibility that sedimentation may have a stabilizing effect by producing an increase in density with decreasing height above the hot plate. The classical analysis of an equilibrium density profile resulting from a balance of sedimentation and Brownian diffusion is usually attributed to Einstein [11]. However, depending on particle size, thermophoresis of particles can also play a major role due to the vertical temperature gradient associated with natural convection.

Classical linear stability analysis of a horizontal fluid layer heated from below assumes a linear temperature gradient, and a corresponding density gradient resulting from thermal contraction of the fluid before initiation of convection. For a colloid suspension there is the possibility of a significant effect on the vertical density gradient resulting from a particle concentration gradient.

The particle concentration equation in a gravity field $-gz$ can be written

$$\frac{\partial n}{\partial t}+u\frac{\partial n}{\partial x}+v\frac{\partial n}{\partial y}+(w+v_S)\frac{\partial n}{\partial z} = \nabla\cdot(D\nabla n+D_T\nabla T n) \tag{A.1}$$

The sedimentation velocity v_S for a spherical particle is given by Stokes Law as

$$v_S=-\frac{(\rho_P-\rho_l)d_P^2 g}{18\mu_l} \tag{A.2}$$

The Brownian diffusion coefficient D is given by

$$D=\frac{k_B T}{3\pi\mu d_P} \tag{A.3}$$

and the thermal diffusion coefficient is related to the thermophoresis velocity v_T as

$$v_T=-D_T\nabla T \tag{A.4}$$

Eq. (A.1) is valid only for small particle concentrations such that the volume fraction ϕ of the particles is negligibly small. Then, for a monodisperse suspension, we can write $\phi=nV_P$ where V_P is the particle volume, and Eq. (A.1) can be written for one dimensional transport as

$$\frac{\partial\phi}{\partial t}+v_S\frac{\partial\phi}{\partial z}=\frac{\partial}{\partial z}\left(D\frac{\partial\phi}{\partial z}+D_T\frac{\partial T}{\partial z}\phi\right) \tag{A.5}$$

Here we have taken $w=0$ consistent with assuming ϕ negligibly small.

The phenomenon of thermophoresis in gases is well understood and can be accurately calculated. However, for liquids the converse is true. Recently Bielenberg and Brenner [12] have published a formulation for thermophoresis in liquids that spans the limits of hydrodynamic and Brownian motion. The model is essentially a hydrodynamic one, developed initially for continuum conditions, and should be valid for the particle sizes of concern in colloids. Unfortunately there is very little experimental data to benchmark the model, and considerable reliance is placed on the experimental data of McNab and Meisen [13] for microsize particles. However, the thermophoretic velocity appears to be independent of particle size so extrapolation to smaller sizes may be appropriate. The thermophoretic velocity can be written as

$$v_T=-C_S\frac{1}{1+\frac{k_P}{2k_l}}\frac{v_l}{T}\nabla T \tag{A.6}$$

where C_S is a constant of order unity. Notice that v_T is temperature dependent, and thus should be evaluated at a mean temperature in Eq. (A.4).

Steady state analysis for long times

The characteristic time for thermal diffusion $t_H=H^2/\alpha$ is much smaller than the characteristic times for particle diffusion, sedimentation and thermophoresis. Thus we

can assume a steady temperature field: for $T = T_1$ at $z = 0$, $T = T_2$ at $z = H$

$$T = T_1 - \frac{z}{H}(T_1 - T_2), \quad (T_1 > T_2) \tag{A.7a}$$

$$\frac{dT}{dt} = -\frac{T_1 - T_2}{H} \quad \text{(negative)} \tag{A.7b}$$

Then $d^2T/dz^2 = 0$: substituting in Eq. (A.5) with D and D_T constant, and a steady state gives

$$(v_S + v_T)\frac{\partial \phi}{\partial z} = D\frac{\partial^2 \phi}{\partial z^2} \tag{A.8a}$$

It is instructive to rewrite this equation as

$$\frac{\partial}{\partial z}\left(-D\frac{\partial \phi}{\partial z} + v_S\phi + v_T\phi\right) = 0 \tag{A.8b}$$

which states that the total particle flux is independent of z

$$\frac{\partial}{\partial z}(J_P) = 0 \tag{A.9}$$

Integrating,

$$J_P = \text{constant} = 0 \tag{A.10}$$

if particles are not deposited on either plate. The assumption of a zero total particle flux was made by Einstein in his analysis of sedimentation–diffusion equilibrium [11]. The hypothesis that particles do not deposit on either wall is not likely to be valid over the complete parameter range. Obviously very large particles will deposit at $z = 0$. But, in general, particle–surface interactions in liquids often prevent deposition. Substituting in Eq. (A.10) and rearranging

$$D\frac{\partial \phi}{\partial z} = (v_S + v_T)\phi \tag{A.11}$$

Let $\eta = z/H$, $\beta = (v_S + v_T)H/D$, then

$$\frac{\partial \phi}{\partial \eta} = \beta\phi \tag{A.12}$$

Integrating with $\phi = \phi_1$ at $\eta = 0$

$$\phi = \phi_1 e^{\beta\eta} \tag{A.13}$$

The average value of ϕ is

$$\bar{\phi} = \int_0^1 \phi\, d\eta = \frac{\phi_1}{\beta}(e^{\beta} - 1) \tag{A.14}$$

Substituting back in Eq. (A.13)

$$\phi = \bar{\phi}\frac{\beta e^{\beta\phi}}{e^{\beta} - 1} \tag{A.15}$$

which is a useful form of the result since $\bar{\phi} = \phi_0$, the initial volume fraction of particles.

The exponential character of the solution indicates that the ϕ profiles will depend on the sign of β, and be very sensitive to $|\beta|$. Thus we now examine values of β that might be encountered in colloid natural convection. Using conditions relevant to our experiments we will take $\Delta T = 10$ K, $H = 6$ mm and $\overline{T} = 20\,^{\circ}C$. Then Eq. (A.6) with $C_S = 0.13$ from McNab and Meisen [13] gives $v_T = 190 \times 10^{-10}$ m/s. The sedimentation velocity is proportional to particle diameter squared. Using Eq. (A.2) $v_S = 6.7 \times 10^{-10}(d_P[\text{nm}]/20)^2$. The Brownian diffusion coefficient is inversely proportional to particle diameter: using Eq. (A.3), $D = 22.3 \times 10^{-12}\ (20/d_P[\text{nm}])$. With these values, Table A.1 shows the pertinent range of β. It is seen that β changes sign at $d_P = 107$ nm. For smaller particle sizes thermophoresis dominates; for larger particle sizes sedimentation dominates. Fig. A.1 shows resulting ϕ profiles calculated from Eq. (A.15). Notice that due to the exponential character of the solution, the behavior changes dramatically as β goes from +10 to −10. The particle size for $\beta = 0$ cannot be calculated with much confidence owing to the uncertainties in the expressions for v_S and v_T, and in practice there is always a distribution of particle sizes around a mean value. However, the important point is that there is some value of d_P for which $v_S = v_T$ and $\beta = 0$, and the behavior changes dramatically on either side of this value.

The density of the suspension is given by Eq. (1) where, owing to the small thermal expansion coefficient of Al_2O_3, ρ_P is taken to be constant at 3970 kg/m^3. The water density $\rho_l(T)$ is taken from Table 11 of Ref. [14]. Fig. A.2 shows $\rho/\rho(z = 0)$ profiles with β as a parameter. For β positive, $d\rho/dz$ is everywhere positive and hence the layer will be unstable for Rayleigh numbers greater than a critical value. For $\beta = 0$, $Ra_{CRIT} = 1708$. For $\beta > 0$, lower values of Ra_{CRIT}

Table A.1
Range of $\beta = (v_S - v_T)H/D_P$ of interest for $\Delta T = 10$ K, $H = 6$ mm; $v_T = 192 \times 10^{-10}$ m/s

d_P [nm]	D_P [m^2/s $\times 10^{12}$]	v_S [m^2/s $\times 10^{10}$]	$v_S - v_T$ [m^2/s $\times 10^{10}$]	β
10	44.6	−1.67	190	2.6
20	22.3	−6.7	185	5.0
40	11.2	−26.8	165	8.9
100	4.46	−167	24	3.3
105	4.25	−184	7	1.0
110	4.06	−202	−11	−1.6
120	3.72	−241	−49	−7.9
150	2.97	−376	−185	−37.2
200	2.23	−669	−478	−128
250	1.78	−1050	−854	−287

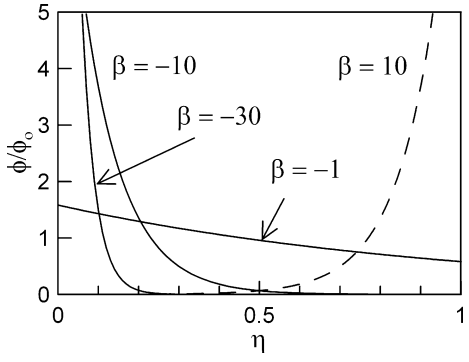

Fig. A.1. Concentration profile for various values of β.

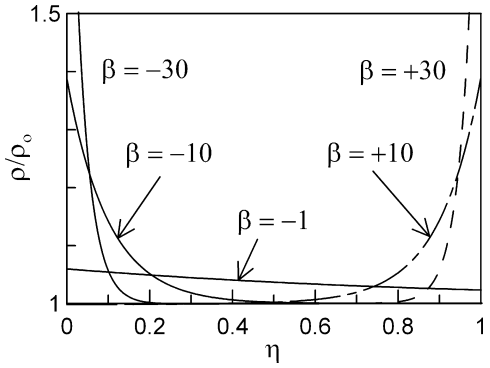

Fig. A.2. Density profiles for various values of β.

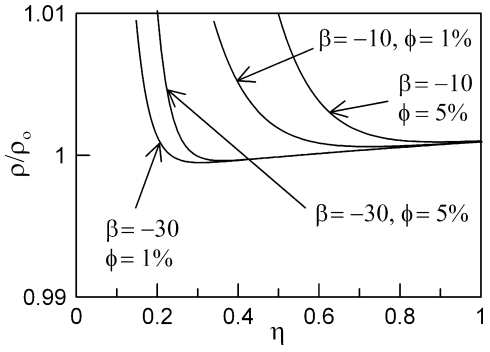

Fig. A.3. Change of density gradient for negative values of β.

might be expected, though the highly nonlinear variation in ρ may yield a complicated dependence of Ra_{CRIT} on β. For β somewhat less than zero, $d\rho/dz$ is everywhere negative and the layer is stable. However, at larger negative values of β, $d\rho/dz$ becomes positive at larger values of η, as shown in Fig. A.3. In this situation the variation in ϕ is negligible at higher values of z and $\rho(z)$ increases due to the contraction of the liquid phase. Thus, the fluid at smaller values of η will be stable, whereas at larger values it will be unstable. There is the possibility of convection developing in the upper layer only, yielding Nusselt numbers lower than would be obtained if no particles were present. Similar phenomena have been obtained in studies of natural convection with larger particles (~50 μm), for example by Chen et al. [15].

The preceding discussion is based on the asymptotic steady state solution of the particle diffusion equation. It gives insight into the roles played by sedimentation, Brownian diffusion and thermophoresis over the particle size range from nano to microparticles. Application of these results to real experiments is made complicated by the very different time scales of vorticity and thermal diffusion on one hand and the particle transport phenomena on the other. The vorticity and thermal diffusion time scales are H^2/ν and H^2/α, respectively. For particle diffusion, thermophoresis and sedimentation, they are H^2/D_P, H/v_T, H/v_S, respectively. Table A.2 shows typical values.

The data presented in Tables A.1 and A.2 together with Figs. A.1–A.3 will now be used to give a qualitative discussion of the effect of particle transport on the critical value of Rayleigh number for initiation of convection in a horizontal fluid layer. Due to the varying time scales involved, it is necessary to carefully specify initial conditions: some specific situations follow:

Case 1. The particle suspension has uniform initial temperature and particle concentration. At time zero the plate temperatures have a step change to T_H at $z = 0$, and T_C at $z = H$, such that the Rayleigh number is less than 1708.

(a) Nanoparticles with $\beta > 0$. The layer will initially be stable for a few minutes as the temperature profile develops to its steady linear form. The layer will remain stable for a number of hours until thermophoresis causes an increase in ϕ and ρ at larger values of η sufficient to destabilize the layer. The critical Rayleigh number will then be less than 1708.

(b) Microparticles with $\beta < 0$. As in case (1a), the layer will be initially stable, but will remain stable as particle sedimentation increases ϕ and ρ at smaller values of η.

Case 2. An initial non-uniform microparticle ($\beta < 0$) distribution resulting from sedimentation occurring for some hours before the plate temperatures are changed to give a $Ra > 1708$ based on properties at $\overline{T}$ and $\bar{\phi}$. It is possible that due to the non-uniform ϕ profile, $d\rho/dz$can be initially negative for all η and the layer stable. But at longer times the variation in ϕ will become negligible at larger values of η giving a positive $d\rho/dz$ due to thermal contraction of the liquid. Thus the fluid at lower values of η can be stable, while at larger values of η can be unstable. There is the possibility of

Table A.2
Characteristic times (h) for $H = 6$ mm, $\Delta T = 10$ K, $\overline{T} = 20$ °C

Particle size [nm]	Vorticity diffusion	Thermal diffusion	Particle diffusion	Thermophoresis	Sedimentation
20	0.01	0.07	224	87	2490
50	”	”	1400	”	400
100	”	”	5600	”	100
150	”	”	1.25×10^4	”	44.3
200	”	”	2.24×10^4	”	24.9
300	”	”	5.04×10^4	”	11.1

convection developing in a layer $\eta^* < \eta < 1$ for which the effective Rayleigh number should be in terms of thickness $H^* = 1 - \eta^*$, and a temperature difference $\Delta T^* = (1 - \eta^*)\Delta T$.

Case 3. As for case 2, but an initial uniform particle concentration. Now it is possible for the layer to become unstable during the initial thermal transient, before there has been sufficient time for sedimentation to stabilize the fluid at smaller values of η. This early development of convection precludes direct application of the analytical results presented here.

Cases 2 and 3 are particularly relevant to the present experimental study for which the results at $\theta = 0°$ show critical Rayleigh numbers as high as 26,000, and reduced Nusselt numbers particularly at lower Rayleigh number. In the experiment, there are two further time scales involved, namely for diffusion of vorticity after the initial mixing of layer, and for the thermal response of the experimental apparatus. These issues are dealt with in the discussion of results in the body of the paper.

References

[1] D. Wen, Y. Ding, Formulation of nanofluids for natural convective heat transfer applications, Int. J. Heat Fluid Flow 26 (2005) 855–864.
[2] D. Wen, Y. Ding, Natural convective heat transfer of suspensions of titanium dioxide nanoparticles (nanofluids), IEEE Trans. Nanotechnol. 5 (2006) 220–227.
[3] N. Putra, W. Roetzel, S.K. Das, Natural convection of nano-fluids, Heat Mass Transfer 39 (2003) 775–784.
[4] K. Khanafer, K. Vafai, M. Lightstone, Buoyancy-driven heat transfer enhancement in a two-dimensional enclosure utilizing nanofluids, Int. J. Heat Mass Transfer 46 (2003) 3639–3653.
[5] X. Zhang, H. Gu, M. Fujii, Effective thermal conductivity and thermal diffusivity of nanofluids containing spherical and cylindrical nanoparticles, Exp. Thermal Fluid Sci. 31 (2007) 593–599.
[6] B.C. Pak, Y.I. Cho, Hydrodynamic and heat transfer study of dispersed fluids with submicron metallic oxide particles, Exp. Heat Transfer 11 (1998) 151–170.
[7] B.H. Chang, A.F. Mills, Natural convection heat transfer in cylindrical enclosure, in: The Sixth ASME–JSME Thermal Engineering Joint Conference TED-AJ03-526, Hawaii, USA, March 16–21, 2003.
[8] H.T. Rossby, A study of Bernard convection with and without rotation, J. Fluid Mech. 36 (1969) 309–336.
[9] K.G.T. Hollands, G.D. Raithby, L. Konicek, Correlation equations for free convection heat transfer in horizontal layers of air and water, Int. J. Heat Mass Transfer 18 (1975) 879–884.
[10] M. Okada, T. Suzuki, Natural convection of water-fine particle suspension in a rectangular cell, Int. J. Heat Mass Transfer 40 (1997) 3201–3208.
[11] A. Einstein, Investigations in the Theory of Brownian Movement, Dover, 1956.
[12] J.R. Bielenberg, H. Brenner, A hydrodynamic/Brownian motion model of thermal diffusion in liquids, Physica A 356 (2005) 279–293.
[13] G.S. McNab, A. Meisen, Thermophoresis in liquids, J. Colloid Interface Sci. 44 (1973) 339–346.
[14] A.F. Mills, Mass Transfer, Prentice Hall, 2001, p. 88.
[15] B. Chen, F. Mikami, N. Nishikawa, Experimental studies on transient features of natural convection in particles suspension, Int. J. Heat Mass Transfer 48 (2005) 2933–2942.